JOURNAL OF MATERIALS SCIENCE 29 (1994) 2826–2834

Corrosion behaviour of aluminium-based metal matrix composites

S. L. COLEMAN, V. D. SCOTT, B. McENANEY
School of Materials Science, University of Bath, UK

The corrosion characteristics, in 3.5 wt% NaCl solution, of aluminium alloy composites containing a range of reinforcements have been investigated using potentiostatic measurements and simple immersion tests. Complementary microstructural studies carried out on corroded surfaces and sections through corroded material have identified a number of preferential corrosion sites; these include the fiber/matrix interface, especially where it contains chemical reaction products resulting from composite fabrication, as well as second phases and pores in the metal matrix. The effect on corrosion behaviour of the different reinforcements, with particular reference to their chemistry and geometry, is discussed, as is the influence of composite manufacturing route.

1. Introduction

The reinforcement of aluminium alloys with either ceramic fibres or particulates is being investigated as a means of improving their stiffness and strength. In parallel with these developments, investigations are being carried out on the effect that these reinforcements may have on other properties of aluminium alloys such as their corrosion resistance. Published literature on the corrosion of aluminium-based composites is, however, rather limited and data which are available tend to concentrate upon the effects produced by carbon and silicon carbide reinforcements. The findings would suggest that the incorporation of reinforcements generally increases corrosion of the aluminium matrix, although the reasons for this are the subject of debate. For example, there is consensus that preferential attack occurs at the reinforcement/matrix interface and, furthermore, that pores, matrix second phases and interfacial reaction products can all influence corrosion behaviour in significant ways. Thus the incorporation of carbon fibres into aluminium alloys is reported to have a detrimental effect upon corrosion because of galvanic interactions between fibre and matrix [1, 2] and the occurrence of Al_4C_3 at the fibre/matrix interface [3–5]. Other data, however, indicate that SiC additions do not appear to affect substantially pitting attack on some aluminium alloys because, whilst pits were more numerous on the composite, they were smaller and shallower than those on unreinforced alloy [3, 6, 7]. Nevertheless, agreement exists that SiC reinforcements can affect corrosion in a less direct way by modifying the microstructure of the matrix alloy when the MMC is being manufactured, firstly by altering the distribution of intermetallic phases [6–9] (affecting galvanic corrosion between intermetallic phases and matrix), and secondly, by introducing residual stresses into the material as a result of differential thermal contraction [10] between reinforcement and matrix.

The present paper focuses upon the response of aluminium-based metal matrix composites (MMC) to a marine environment and sets out to identify, separately where possible, the influence of ceramic reinforcement, matrix chemistry and composite manufacturing route on corrosion behaviour.

2. Experimental procedure

2.1. Materials

The matrix metals used in the investigation were Al–7Si–0.5Mg casting alloy (designated 357) and Al–4Cu–1.5Mg wrought alloy (designated 2124). Several types of reinforcement were studied: (a) carbon (Courtaulds Ltd, UK), a PAN-based continuous 8 μm diameter fibre, (b) Nicalon (Nippon Carbon Ltd, Japan), a continuous 15 μm diameter fibre based upon SiC, (c) Saffil (ICI Ltd, UK), a short 3 μm diameter fibre of δ–Al_2O_3 and (d) particulate silicon carbide, $\sim$ 3 μm diameter.

Fibre-reinforced composites were fabricated by liquid metal infiltration of a fibre preform, either assisted by applying inert gas at a low pressure of $\sim$ 5 MPa, or by squeeze casting at the higher pressure of $\sim$ 40 MPa. With carbon and Nicalon preforms infiltrated using the low-pressure method, a glass fibre weft was used to support the fibre. With the squeeze-cast material, carbon fibres were wound upon an aluminium former and the whole assembly positioned in the die prior to infiltration. The Saffil fibre was supplied in the form of a porous preform containing silica binder and was suitable for direct infiltration. The particulate-reinforced composite was made by a powder metallurgy route and supplied (BP Ltd, UK) as 3 mm thick sheet. Table I lists the composite systems, their method of fabrication and their designation; the letters L and H are used to identify carbon fibre-reinforced 357 composites made by low-pressure and high-pressure infiltration, respectively.

0022–2461

TABLE I Designation and details of materials used in the investigation

Designation	Reinforcement and arrangement	Fabrication[a]
357	Unreinforced alloy	
357-Saf	Short alumina fibre (Saffil), planar random	LP
357-Nic	Continuous SiC-based fibre (Nicalon), unidirectional	LP
357-C(L)	Continuous carbon fibre, 0°/90° crossply	LP
357-C(H)	Continuous carbon fibre, unidirectional	HP
2124	Unreinforced alloy	
2124-C	Continuous carbon fibre, unidirectional	HP
2124-SiC	Particulate, random	PM

[a]LP, liquid metal infiltration using low gas pressure, ~ 5 MPa.
HP, liquid metal infiltration using external pressure, ~ 40 MPa (squeeze casting).
PM, powder metallurgy.

Studies were carried out on all composites in the as-fabricated condition, on unreinforced 357 alloy in the cast condition and on 2124 alloy in the T851 condition (heat-treated and strained 2%).

2.2. Specimen preparation

Metallographic preparation of corrosion test specimens was as follows. Specimens of composite and unreinforced material were cut into $\sim 10 \times 10 \times 5\,mm^3$ pieces using an abrasive cutting wheel. Transverse sections (perpendicular to the fibre direction) were prepared from unidirectionally reinforced material, 357-C(H), 357-Nic and 2124-C, whilst sections of the cross-ply composite, 357-C(L), exposed fibres in the transverse and longitudinal directions simultaneously. Discontinuously reinforced materials, 357-Saf and 2124-SiC, had randomly cut sections. All specimens were mounted in epoxy resin and polished using successively finer sizes of diamond to achieve a smooth surface.

Microstructures of prepared surfaces were studied by scanning electron microscopy (SEM) and the chemical composition of microstructural features determined using the energy-dispersive spectrometer (EDS) fitted to the microscope.

2.3. Corrosion tests

Corrosion experiments were performed at 25 °C in 3.5 wt % NaCl solution prepared from a mixture of reagent grade NaCl and distilled water. The solution was deaerated by purging with nitrogen gas for 1 h prior to and during specimen immersion, except when carrying out the galvanic tests.

2.3.1. Double cyclic polarization tests

The double cyclic polarization (DCP) test method, as used by Otani *et al.* [8, 9] and further developed by the present authors [11], was adopted because it provided a more clearly defined measurement of the pitting potential compared with a single cyclic polarization test. The sample was first positioned in a PTFE holder to expose a specimen area of 100 mm^2 and the whole assembly immersed in the solution for ~ 10 min prior to polarization. A scan rate of 20 $mV\,min^{-1}$ was used, this having been shown [11] to give results which were in close agreement with those produced using ASTM standard G5-78. At the start of the first cycle, a potential ~ 500 mV below the rest potential was applied to the specimen and this was increased until a maximum current density of 5 $mA\,cm^{-2}$ was attained. At the end of the forward scan the direction of the potential was reversed until the initial potential was reached. A second identical cyclic polarization was then performed immediately following the first. Three DCP tests were carried out on each material and mean values for the pitting and corrosion potentials were taken from the second cycle. The reproducibility between tests was found to be typically ± 10 mV for the pitting potential and ± 50 mV for the corrosion potential.

2.3.2. Galvanic tests

Measurements were performed on couples consisting of unreinforced matrix metal and fibre, either of carbon or Nicalon in the form of tows. Bare fibres were placed in the salt solution and connected to the metal via a zero-resistance ammeter. The galvanic current flowing between fibres and metal was then recorded over a 2 h period.

2.3.3. Simple immersion tests

Samples were immersed in salt solution for periods up to 3 weeks. At the end of a test they were cleaned in 10% HNO_3 for ~ 10 min, rinsed in distilled water and dried. The corroded surface microstructure was studied by optical microscopy and SEM, with EDS being used to establish the chemical composition of salient microstructural features.

The gravimetric method of determining corrosion rates, that is by weighing samples before and after prescribed periods of immersion, presented problems because the extensive pits, which characterized the response of MMC to corrosion, tended to retain reaction products and give unrealistic measurements. It was, therefore, decided to estimate the extent of corrosive attack by carrying out SEM studies of cross-sections through corroded specimens and recording the maximum depth of corrosion. Samples subjected to 3 weeks immersion were used for this purpose.

3. Results

3.1. Double cyclic polarization tests

Fig. 1 is a polarization curve from Saffil-reinforced 357 alloy. It shows pitting potentials on both cycles (a and b, respectively), but a more clearly defined value on the second cycle. The corrosion potential on the second

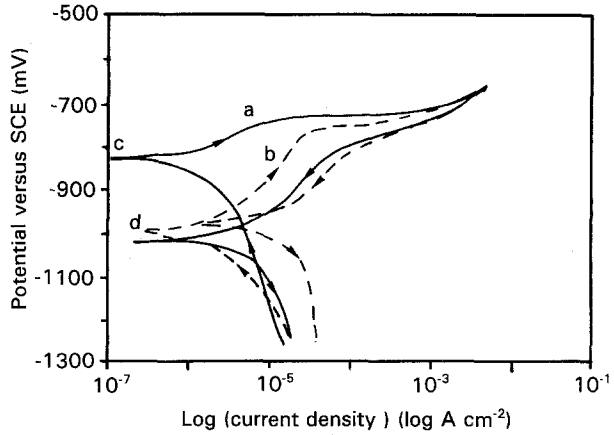

Figure 1 DCP curve for 357-Saf; pitting potentials (a, b) and corrosion potentials (c, d) on (——) first and (– – –) second cycles.

cycle (point d) was much more negative than that on the first cycle (point c). The mean values for pitting potential and corrosion potential, as recorded on the second cycle, were − 761 and − 938 mV, respectively. The form of the polarization curve was somewhat different for the Nicalon-reinforced composite, 357-Nic, Fig. 2. The pitting potential could not be distinguished at all on the first cycle because it was closely similar to the corrosion potential. Also, above E_{corr}, the increase in current density with applied potential was more pronounced than that shown in Fig. 1. Mean values for pitting and corrosion potentials taken from the second cycle for 357-Nic were − 751 and − 969 mV, respectively.

All the materials investigated could be placed in one or other of these two categories of behaviour, which we shall term type A (Fig. 1) and type B (Fig. 2). Unreinforced 357 alloy and 357-C(H) composite showed type A behaviour, whilst type B curves were obtained on 2124 alloy, 357-C(L), 2124-C and 2124-SiC composites, see Table II. Values of pitting potential and corrosion potential for all materials are also given in Table II. The data indicate that composites based upon 357 alloy gave more negative pitting potentials than the unreinforced metal, which suggests that the reinforcements increase the susceptibility of 357 alloy to pitting. In the 2124-based composites,

TABLE II Polarization data from DCP tests

Material	E_{pit}(mV)	E_{corr}(mV)	Behaviour type
357	− 743	− 995	A
357-Saf	− 761	− 938	A/B
357-Nic	− 751	− 969	B
357-C(L)	− 752	− 919	B
357-C(H)	− 763	− 880	A
2124	− 748	− 1047	B
2124-C	− 705	− 958	B
2124-SiC	− 726	− 1147	B

pitting potentials appeared, however, to be more positive than that recorded on unreinforced metal, a point to which we shall return in Section 4.4.

3.2. Galvanic tests

Values of galvanic current measured between metal and fibre are reported in Table III. Couples involving carbon fibres produced the greatest galvanic current with the 357/carbon and 2124/carbon systems giving 465 and 320 μA, respectively. The 357/Nicalon couple gave a current of 72 μA.

3.3. Simple immersion tests

3.3.1. 357

During the first hour of immersion, signs of pitting were observed at second phases, Fig. 3; they were found using SEM/EDS to be iron-rich and identified

TABLE III Galvanic corrosion rates for metal/conductive fibre couples

Metal	Fibre	Current (μA)
357	carbon	465
357	Nicalon	72
2124	carbon	320

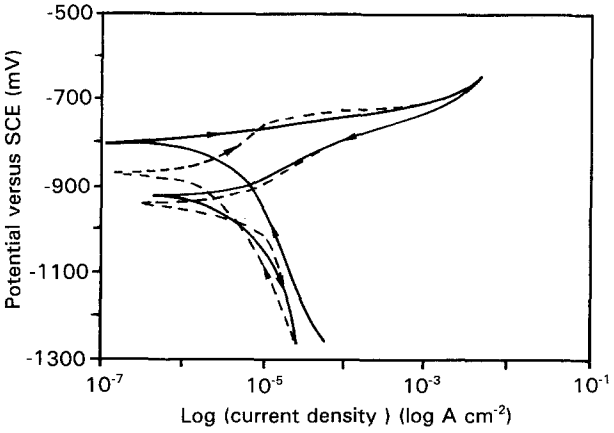

Figure 2 DCP curve for 357-Nic. (——) First cycle, (– – –) second cycle.

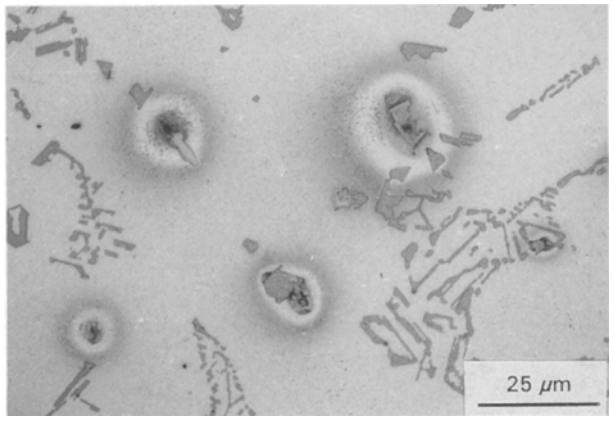

Figure 3 Corrosion at iron-rich intermetallics in unreinforced 357 alloy; immersion for 1 h.

as the intermetallics $Al_8Si_6Mg_3Fe$ and Fe_2SiAl_8. After 1 day, corrosion was observed also at silicon particles contained within the eutectic structure. Following 3 weeks immersion, the aluminium dendrites suffered general attack, sections through the specimen showed that corrosion had penetrated up to $\sim$ 45 μm into the material, see Table IV.

3.3.2. 357-Saf

After immersion for 1 day, localized attack of matrix regions around particles of $FeSiAl_5$ was clearly visible. More of these corrosion centres were present in the composite than in the unreinforced alloy. The extent of attack remained virtually unchanged for 3 days but after 3 weeks, pits had also developed in matrix regions surrounding fibres and silicon particles, Fig. 4a. Cross-sections through the corroded surface, Fig. 4b, showed the pits had a maximum depth of $\sim$ 35 μm.

3.3.3. 357-Nic

Pitting during the first day of immersion again occurred at the $FeSiAl_5$ intermetallics but also at the Nicalon fibre/matrix interface, particularly in regions of incomplete infiltration around the glass weft. Following 3 weeks immersion, matrix regions became extensively corroded, Fig. 5, especially at the glass weft where the depth of attack reached $\sim$ 350 μm.

3.3.4. 357-C(L)

During the first day of immersion, localized matrix corrosion occurred adjacent to $FeSiAl_5$ intermetallics and a plate-like phase of approximate composition FeCrSiAl. Attack was pronounced at the carbon fibre/matrix interface, particularly where pores were present due to incomplete infiltration of the composite, and a few cracks were observed within the tows to follow the carbon fibre/matrix interface. The severity of attack progressively increased over the following few days until, after 3 weeks, the cracks within carbon fibre tows had opened up to form crevices $\sim$ 30–40 μm wide. A region taken from a polished cross-section through the corroded sample is illustrated in Fig. 6 The manner in which the fibres appear to have been forced apart is evidence of the presence of stress, probably a combination of residual stress in the composite and that produced by the volume expansion accompanying the formation of corrosion products within the specimen. The depth of corrosion was generally < 25 μm, although some localized attack at the edge of carbon fibre tows was noted, in one case completely penetrating the $\sim$ 6 mm thick specimen.

TABLE IV Maximum depth of corrosive attack after immersion for 3 weeks

Material	Depth of corrosion (μm)
357	45
357-Saf	35
357-Nic	350
357-C(L)	6000
357-C(H)	300
2124	35
2124-C	50
2124-SiC	40

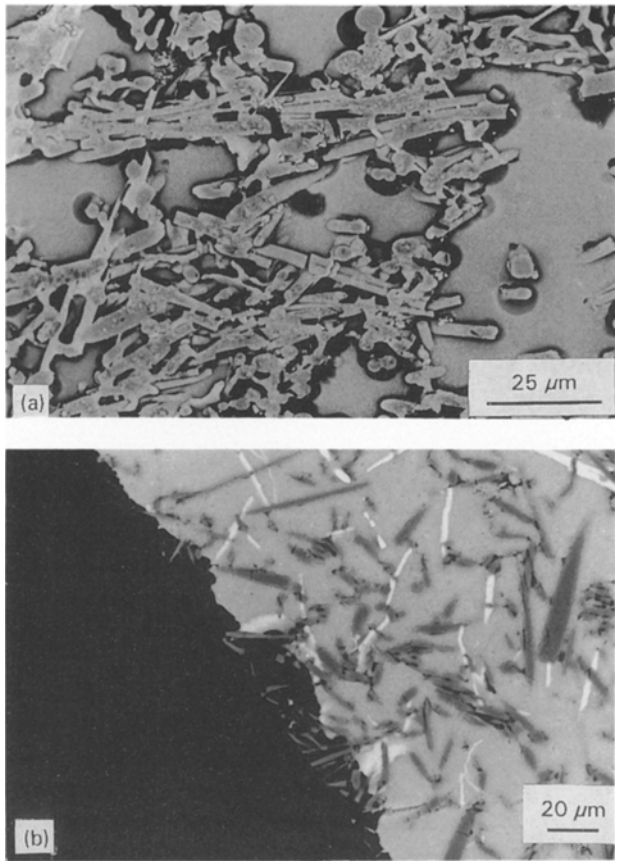

Figure 4 Corrosion of 357-Saf after 3 weeks immersion; (a) corroded surface, and (b) cross-section through corroded surface.

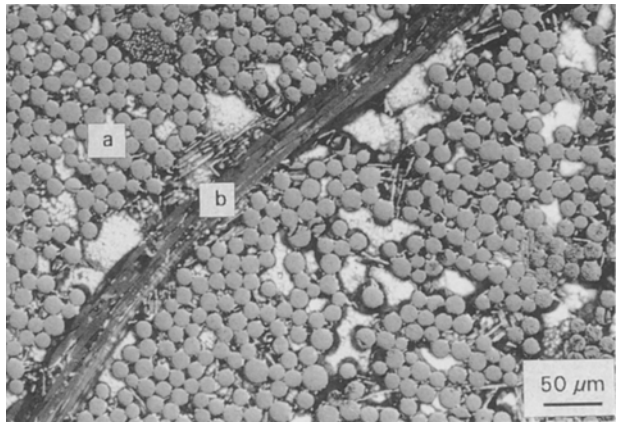

Figure 5 Corrosion of 357-Nic following immersion for 3 weeks, showing attack on matrix surrounding Nicalon fibres (a) and glass binder (b).

3.3.5. 357-C(H)

Corrosion was slight after the first day of immersion, with a few pits situated mostly at particles of silicon

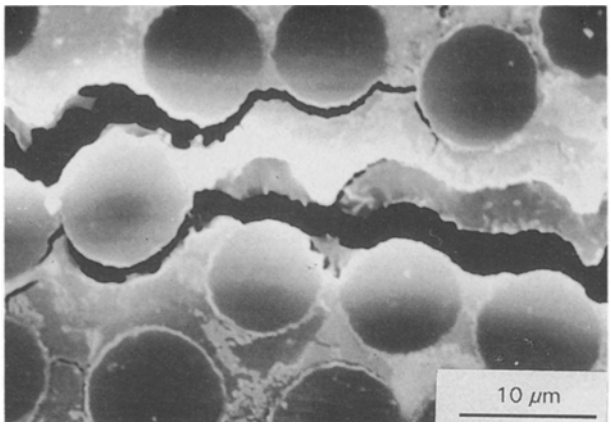

Figure 6 Internal cracking in corroded 357-C(L); immersion for 3 weeks.

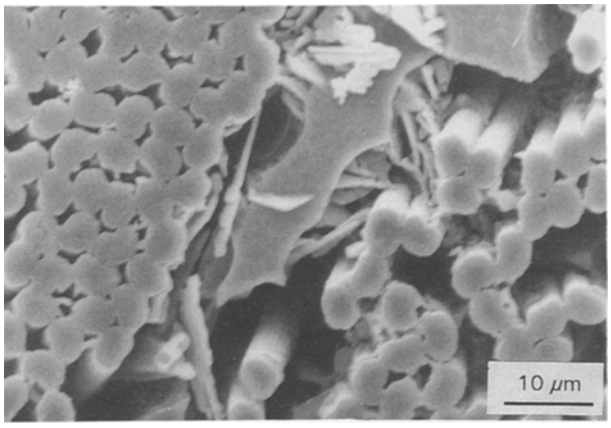

Figure 7 Corrosion around fibres and second phases in 357-C(H) after 3 weeks immersion.

and $FeSiAl_5$. After 3 days, corrosion at the second phases was more severe and, after 3 weeks immersion, much of the matrix had suffered corrosion, Fig. 7. Cross-sections through the material showed the depth of attack to be ~ 95 μm over most of the surface, with a few localized sites where corrosion extended to ~ 300 μm.

3.3.6. 2124

During the first day of immersion many corrosion sites had formed, significantly more than were observed on unreinforced 357 alloy. Examination of a specimen after immersion for 3 days showed substantial attack of the matrix surrounding an iron-rich phase identified as $(CuFeMn)Al_6$, but little at the phase, Al_2CuMg. After 3 weeks, corrosion around both types of second phases had increased so much that they became detached from the surface, Fig. 8; the "corrosion grooves" are evidence of the strong texture possessed by the metal due to cold work. The maximum pit depth recorded from cross-sections through the corroded surface was 35 μm.

3.3.7. 2124-C

During the first day of immersion, preferential attack was noted at fibre/matrix interfaces and $(CuFeMn)Al_6$,

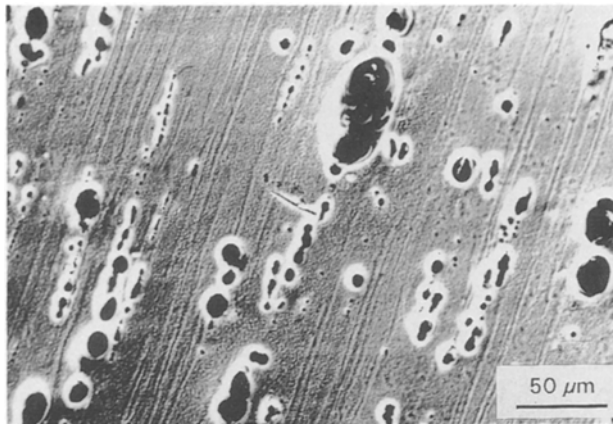

Figure 8 Detachment of second phases from the surface of 2124 alloy after 3 weeks immersion.

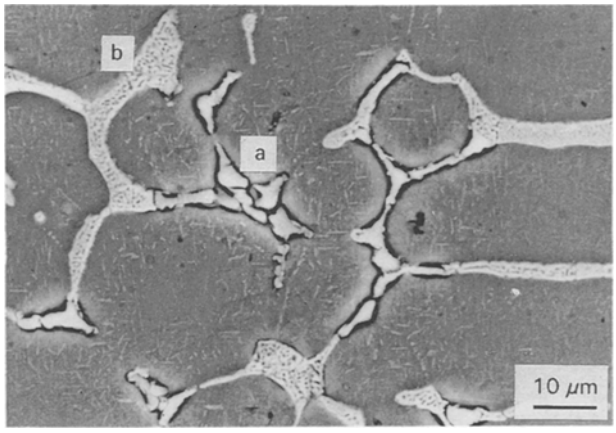

Figure 9 Corrosion of 2124-C (matrix-rich region); immersion for 3 days showing attack adjacent to $(CuFeMn)Al_6$ (a), but no attack associated with $CuMgAl_2$ (b).

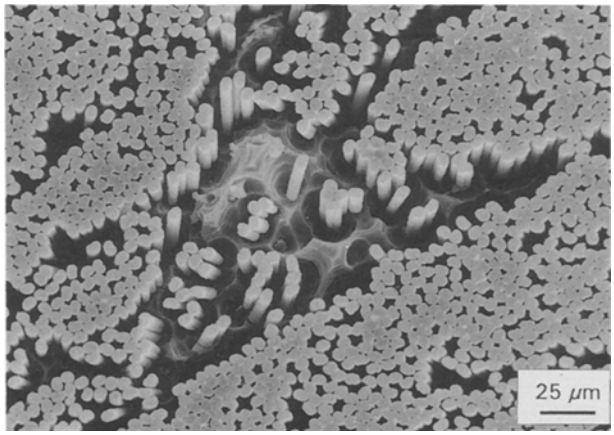

Figure 10 Corrosion of 2124-C; immersion for 3 weeks.

Fig. 9, but as with unreinforced metal, the matrix regions surrounding the Al_2CuMg phase suffered little corrosion. After 3 days, attack around the intermetallics had increased as had the number of pits developed at fibre/matrix interfaces; a deposit was found around some of the fibres and shown by EDS to contain copper. Following corrosion for 1 week, the intermetallic phases became detached from the matrix and,

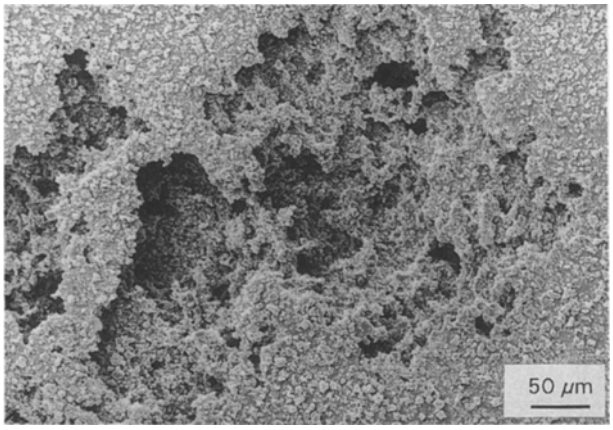

Figure 11 Pits developed in 2124-SiC after 3 weeks corrosion.

after 3 weeks immersion, most of the matrix exhibited corrosion, Fig. 10. At this stage, sufficient deposit had formed in some regions to allow it to be identified as essentially copper. The depth of corrosion extended to ~ 50 μm.

3.3.8. 2124-SiC

After immersion for 1 day, small corrosion pits were observed at particles of $(CuFeMn)Al_6$ and $CuAl_2$. Pits were present close to the silicon carbide particulates although closer inspection revealed that these were also associated with intermetallics. The pits grew progressively in size until, after 3 weeks immersion, they covered most of the surface, Fig. 11, with a depth of up to ~ 40 μm.

4. Discussion

4.1. General corrosion characteristics

It was found that two types of polarization curve, here designated A and B, were obtained from double cyclic polarization (DCP) tests carried out in salt water, and that polarization data obtained on all the materials investigated in the present programme could be placed in either one of these categories. Materials with type A characteristics exhibited pitting potentials on both cycles, behaviour which is consistent with "classical" cyclic polarization whereby the sample becomes passivated at the start of the test and localized corrosion does not begin until the pitting potential is reached. However, in the present work, the pitting potential is somewhat less well defined on the first cycle, which suggests that the sample had not become completely passivated at the start of the test and that a few corrosion sites remained active. With type B materials the pitting potential was not visible on the first cycle, the rapid increase in current density normally associated with the onset of pitting occurring at the corrosion potential. Thus E_{pit} was defined on the second cycle only. This behaviour suggests that, despite specimen polarization to cathodic potentials at the start of the test, pits which formed prior to polarization remained active until the latter part of the first cycle. Thereafter, pits were deactivated under the applied cathodic potential such that the second cycle followed "classical" cyclic polarization behaviour [11]. Thus while pits grew on all materials, they were more easily de-activated on those which exhibited type A characteristics, from which it follows that such materials were subject to less severe corrosion.

Unreinforced 357 alloy (Al–7Si–0.5Mg) provided a good example of type A behaviour, those pits that were developed being localized at second phases in the material such as iron-rich intermetallic particles. On the other hand, unreinforced 2124 alloy (Al–4Cu–1.5 Mg) showed type B characteristics and here there were many more second phases present, such as copper-rich intermetallics of the type Al_2CuMg, which could act as sites for corrosion attack. The DCP data demonstrated that the different reinforcements affected the corrosion behaviour of these two aluminium alloys in different ways, as the following discussion shows.

4.2. Effect of reinforcement

DCP results show that the addition of Nicalon fibres to 357 alloy resulted in the corrosion characteristics being changed from type A to type B behaviour. This is in accord with the marked increase in the depth of corrosion pits, from a maximum value of 45 μm in unreinforced alloy to values greater than 300 μm in the composite. The two 357-based composites containing carbon fibres showed, however, contrasting behaviour. That manufactured by low-pressure metal infiltration, 357-C(L), exhibited type B behaviour, whereas that produced using high-pressure infiltration, 357-C(H), showed type A characteristics. With Saffil-reinforced 357 alloy, type A characteristics were generally exhibited, possibly as a consequence of the inert nature of the alumina-based Saffil fibre. Corrosion effects which may be attributed directly to the method of composite fabrication are discussed in Section 4.4.

With composites based upon 2124 alloy, the effects of adding reinforcements of carbon or silicon carbide were not so obvious from the form of the DCP curves because all three materials exhibited type B behaviour. Moreover the maximum depth of corrosion pits on these materials did not differ significantly from each other.

Studies of composites immersed for prescribed periods clearly showed localized corrosion taking place at the reinforcement/matrix interface, the degree of reaction being a function of the fibre/matrix combination. It is probable that the interface provided a preferential site because of the likely discontinuity in the surface oxide film due to the changed substrate structure. Such a discontinuity would facilitate the passage of chloride ions to the metal which, once contacted by ions, would suffer localized corrosion. Thereafter electrochemical and microstructural factors would come into play.

The electrochemical factor contributing to interface corrosion involves the development of a galvanic current between a conductive fibre and a metal matrix. Thus the galvanic current of 465 μA recorded on the 357/carbon couple indicates a greater corrosion rate

than that for the 357/Nicalon couple with its galvanic current of 72 μA (Table III). These data correlate with the maximum pit depths of 6.0 and 0.35 mm, measured in the respective composites (Table IV). For the 2124/carbon couple, however, a galvanic current of 320 μA was recorded, although the pit depth in the corresponding MMC was only 0.05 mm. Thus although galvanic currents and pits depths are measures of corrosion activity in the composite, it would appear that other factors have influenced corrosion at the fibre/matrix interface, such as the presence of an additional phase.

Indeed, there is much detailed microstructural evidence showing that second phases caused by chemical reaction between fibre and matrix may be present at the interface. For example, interfacial aluminium carbide is a common occurrence in carbon fibre-reinforced 357 alloy manufactured by the low-pressure infiltration process [12]. Also, aluminium carbide has been found in Nicalon-reinforced MMC made by the same low-pressure route [13], although rather less was present in this case. These composites were the same two materials, 357-C(L) and 357-Nic, as used in the present corrosion studies. The other two continuous fibre-reinforced composite materials investigated here, 357-C(H) and 2124-C, were also found, by TEM examination, to contain interfacial aluminium carbide. Fig. 12 shows the growth of an aluminium carbide crystal from the fibre surface into the metal matrix for a distance of more than 200 nm. Quantitative estimates of the amount of carbide present in the four composites were difficult to achieve but it was possible to place them in order of increasing carbide content: 2124-C, 357-C(H), 357-Nic and 357-C(L). Now it is well known that aluminium carbide readily hydrolyses upon immersion in water and, consequently, the amount of carbide present in a composite would be a contributory factor to the extent of corrosive attack. Accordingly, the depth of corrosion pit in the four materials followed the same trend as the aluminium carbide content, i.e. 50, 300, 350 and 6000 μm, respectively. It is also apparent that not only fibre type (carbon or Nicalon) influences aluminium carbide formation, but also the method of fabricating the composite, a factor to be considered further in Section 4.4.

Finally, the geometrical arrangement of the reinforcement appeared to influence corrosion. In the case of MMC reinforced with continuous fibres, corrosion was generally channelled along the fibres to form corrosion pits deep within the material; this was particularly marked in regions where fibres were closely packed together and porosity was present. In MMC reinforced with short Saffil fibre and particulate silicon carbide, pit depths were similar to those in the respective unreinforced alloys, indicating that the geometrical arrangement of these reinforcements had little influence on the propagation of corrosion pits.

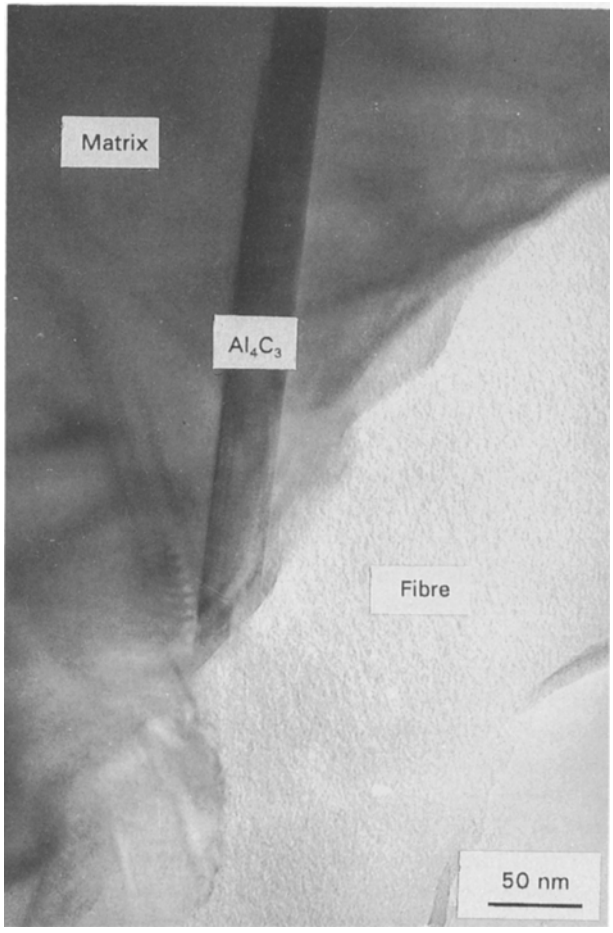

Figure 12 Aluminium carbide at fibre/matrix interface in 2124-C material.

4.3. Effect of matrix chemistry

Alloying elements, such as silicon in 357 alloy and copper in 2124 alloy, had a pronounced effect upon the corrosion characteristics of the composites. This was partly due to solid solution effects but mainly because of the matrix second phases which were formed, either from the alloying additions or from adventitious impurities picked up during composite fabrication. These phases had a more electropositive (cathodic) potential than the matrix and, consequently, corrosion of the surrounding matrix was promoted by galvanic action. The process would be further encouraged by a less protective surface oxide at the second phases [14] which would then lead to film breakdown, exposure of the substrate, and the commencement of corrosion.

The eutectic phase in 357 alloy consisted essentially of pure silicon surrounded by pure aluminium, the galvanic current between these two constituents leading to corrosion at the aluminium/silicon interface whether or not reinforcements were present. A more aggressive reaction occurred at intermetallic particles, particularly those containing iron, such as $FeSiAl_5$, a contaminant introduced during manufacture of the composite. This was evinced in 357-based composites fabricated by low-pressure infiltration and was especially marked in 357-Saf, where severe matrix corrosion adjacent to the intermetallic phase occurred several days earlier than regions next to the relatively inert fibres.

The deleterious nature of iron-containing intermetallics was evinced also in 2124-C composites,

where significant corrosion of the matrix surrounding the phase $(CuFeMn)Al_6$ occurred after 1 day immersion, whereas the normal equilibrium phase, Al_2CuMg, remained relatively inactive even after 3 days; see Fig. 3. In the case of the particulate-reinforced composite, 2124-SiC, the matrix surrounding the iron-containing phase, $(CuFeMn)Al_6$, was again severely attacked, as was that surrounding the $CuAl_2$ phase. (The absence of magnesium in second phases in 2124-SiC could be due to magnesium leaching during hot rolling).

The deposition of copper around some fibres in 2124-C composite after 3 days immersion agrees with the findings of Summerson and Sprowls [15] who noted that copper ions could be plated out on an aluminium surface to create small galvanic cells and intensify pitting. This could explain why the 2124-C composite did not exhibit extensive attack in fibre regions until later stages of immersion.

4.4. Effect of fabrication

The method of manufacturing a composite affects its microstructure in a number of ways. For example, the temperature and time involved in the process would affect the extent of chemical reaction between fibre and matrix and also the form and distribution of matrix second phases, whilst the pressure applied would influence porosity. Thus the carbon fibre-reinforced 357 alloy made by high pressure infiltration contained less interfacial aluminium carbide than that made by low-pressure infiltration because it was held at high temperature for 2 min compared with 15 min. This explains why 357-C(H) showed smaller pit depths (300 μm maximum) and less active (type A) DCP behaviour compared with the deep pits (up to 6000 μm) and more active DCP characteristics (type B) of 357-C(L) material. It is also evident that porosity has contributed to the development of corrosion pits in the composite. For example, 357-C(H) contained less porosity than 357-C(L) due to the higher pressure used in its fabrication, ~ 40 MPa compared with ~ 5 MPa and suffered less severe corrosion attack. It should be remarked that porosity in 357-C(L) was due partly to the glass binder which restrained the carbon fibres during infiltration and restricted the penetration of liquid metal. Thus it is our contention that porosity as well as the presence of aluminium carbide at the fibre/matrix interface have acted as wicks for the corrosion solution to penetrate deeply within the composite within a relatively short period of time.

DCP data on 357-based materials showed that the composites, all of which were made by a casting route, had more negative pitting potentials (ranging from -751 to -763 mV) than the unreinforced alloy (-743 mV) although, in view of the experimental error, it is difficult to discriminate between the values obtained on the composites. It may be concluded, therefore, that because all composites had similar pitting potentials, the type of reinforcement – conductive carbon, semi-conductive Nicalon or non-conductive Saffil – was not the most significant factor. Indeed, a common feature of the composites was the initiation of corrosion pits at iron-containing intermetallics, which would account for their similar pitting potentials. It therefore follows that because the iron was introduced during manufacture of the composite, the processing route has been the major factor which has influenced the pitting potential of this group of materials.

However, whilst the reinforcement does not appear to affect directly the initial corrosion behaviour when pits start to develop, it does affect the subsequent course of corrosion as other microstructural features come into play. For example, the interfacial aluminium carbide, a consequence of the particular fibre/matrix combination, can become the dominant influence on corrosion and eventually lead to the extensive penetration seen in carbon fibre-reinforced materials such as 357-C(L).

In contrast, each of the 2124-based materials was fabricated by a different process; the unreinforced alloy was studied in the T851 heat-treated condition, the 2124-C composite was in the cast condition and the 2124-SiC composite had been fabricated by a powder metallurgy route. Consequently, it was not surprising to observe more variability in the values of E_{pit} recorded on 2124-based composites than those measured on 357-based composites, because the latter group of materials had been produced by a casting route. The fact that unreinforced 2124 alloy had a more active potential (-748 mV) than either the 2124-SiC (-726 mV) or 2124-C (-705 mV) composites accords with the data of Galvele *et al.* [16] who reported that heat treatment of Al–Cu alloys caused the pitting potential to move to more negative values.

5. Conclusion

Salt-water corrosion of the composites was concentrated at interfaces associated with matrix second phases, such as iron-rich intermetallics, and aluminium carbide; imperfections in the surface oxide at interface regions were believed to initiate corrosion at these sites. Once corrosion was initiated, galvanic effects came into play. The method of fabricating the composite influenced the distribution and the extent of these second phases, the iron-rich intermetallics resulting from impurities introduced during manufacture and the aluminium carbide from chemical reaction between fibre and matrix during the high-temperature processing stage. Reinforcement geometry influenced the propagation of corrosion pits, continuous fibres tending to channel corrosion deep within the MMC compared with short fibres and particulates which had little effect. Porosity in the composite, which was accentuated by the use of a glass fibre binder, intensified localized corrosive attack deep within the composite.

These observations stress the importance of taking into account the total composite system, that is the method of fabricating the composite as well as the fibre/matrix combination, when considering MMC corrosion behaviour.

Acknowledgements

This work has been carried out with the support of the SERC and the Defence Research Agency, Holton Heath.

References

1. C. M. FRIEND, C. NAISH, T. M. O'BRIEN and G. SAMPLE, in "Fourth European Conference on Composite Materials", edited by J. Füller, G. Grüninger, K. Schulte, A. R. Bunsell and A. Massiah (Elsevier, London, New York, 1990) p. 307.
2. M. SAXENA, O. P. MODY, A. H. YAGNESHWARAN and P. K. ROHATGI, *Corros. Sci.* **27** (1987) 249.
3. D. M. AYLOR and P. J. MORAN, *J. Electrochem. Soc.* **132** (1985) 1277.
4. J. M. EVANS and D. M. BRADDICK, *Corros. Sci.* **11** (1971) 611.
5. R. B. BHAGAT, M. F. AMATEAU, J. C. CONWAY Jr, J. M. PAULICK, J. M. CHISHOLM, J. M. PARNELL and D. G. SEIDENSTICKER, *J. Compos. Mater.* **23** (1989) 961.
6. P. P. TRZASKOMA, E. McCAFFERTY and C. R. CROWE, *J. Electrochem. Soc.* **130** (1983) 1804.
7. P. P. TRZASKOMA, *Corrosion* **46** (1990) 402.
8. T. OTANI, B. McENANEY and V. D. SCOTT, in "International Symposium on Cast Reinforced Metal Composites", edited by S. G. Fishman and A. K. Dhingra (ASM International, Philadelphia, PA, 1988) p. 383.
9. *Idem*, in "7th International Conference on Composite Materials", Vol. I, edited by Wu Yunshu, Gu Zhenlong and Wu Renjie (International Academic, Beijing, 1989) p. 423.
10. R. C. PACIEJ and V. S. AGARWALA, *Corrosion* **44** (1988) 680.
11. S. L. COLEMAN, B. McENANEY and V. D. SCOTT, *Br. Corros. J.* **26** (1991) 186.
12. MING YANG and V. D. SCOTT, *J. Mater. Sci.* **26** (1991) 1609.
13. A. R. CHAPMAN, V. D. SCOTT and MING YANG, in "8th International Conference on Composite Materials", edited by S. W. Tsai and G. S. Springer, (SAMPE, Covina CA, 1991) 19G, p. 1.
14. G. A. W. MURRAY, H. J. LAMB and H. P. GODARD, *Br. Corros. J.* **2** (1967) 216.
15. T. J. SUMMERSON and D. O. SPROWLS, in "International Conference on Aluminium Alloys–Physical and Chemical Properties", Vol. 3, edited by E. A. Starke Jr and T. H. Sanders Jr (EMAS, Warley Heath, West Midlands, 1986) p. 1575.
16. J. R. GALVELE, S. M. de MICHELI, I. L. MULLER, S. B. de WEXLER and I. L. ALANIS, in "Localised Corrosion", edited by R. Staehle, B. Brown, J. Kruger and A. Agrawal (NACE, Houston TX, 1974) p. 580.

Received 22 October 1993
and accepted 6 January 1994